Available online at www.sciencedirect.com
SCIENCE DIRECT®
Journal of Molecular Catalysis A: Chemical 212 (2004) 251–257
JOURNAL OF MOLECULAR CATALYSIS A: CHEMICAL
www.elsevier.com/locate/molcata

Heterogeneous basic catalysts for the transesterification and the polycondensation reactions in PET production from DMT

M. Di Serio, R. Tesser, A. Ferrara, E. Santacesaria*

Dipartimento di Chimica, Università di Napoli Federico II, via Cintia, 80126 Naples, Italy

Received 10 June 2003; received in revised form 29 October 2003; accepted 30 October 2003

Abstract

The use of heterogeneous basic catalysts in both dimethyl terephthalate (DMT) transesterification with ethylene glycol (EG) and successive polycondensation of the obtained prepolymer, was investigated. To this end, Al_2O_3, calcined Al–Mg hydrotalcite with different Al/(Al + Mg) theoretical atomic ratios, and MgO were tested in transesterification and polycondensation reactions and characterised. It was shown that both the calcined Al–Mg hydrotalcites and magnesium oxides are active in the DMT transesterification reaction with EG and in the successive prepolymer polycondensation. The observed activities were compared to the results of characterisations of catalysts. Moreover, the obtained PETs have chemical and physical properties very close to those of commercial samples.

Keywords: Transesterification; Polycondensation; Dimethyl terephthalate; Poly(ethylene terephthalate); Heterogeneous catalysts

1. Introduction

Poly(ethylene terephthalate) (PET) is largely used for the production of films, plastic objects and fibres. The production of PET is normally carried out in two stages: (i) prepolymer synthesis which is mainly bis(2-hydroxyethyl) terephthalate (BHET); and (ii) a polycondensation stage.

The prepolymer is synthesised either through the esterification of terephthalic acid (TPA) and ethylene glycol (EG) or through the transesterification of dimethyl terephthalate (DMT) and EG. The transesterification reaction is promoted by homogeneous catalysts such as zinc, manganese, lead acetates, and many others, used alone or in mixtures [1,2]. Transesterification is performed at 150–200 °C and the methanol released during the reaction is removed by distillation from the reaction mixture.

In the second stage, the prepolymer is polymerised at higher temperatures (250–290 °C) using a high vacuum and the EG formed is continuously removed. All the catalysts used for transesterification could catalyse the polycondensation because the two reactions are quite similar, but these catalysts do not provide satisfactory products because they are also active in ester decomposition [3,4]. Therefore, in practice, the transesterification catalyst is sequestered using an opportune additive, and a different polycondensation catalyst, mainly an antimony compound, is introduced for the second stage [4]. The antimony compounds cannot be used in the first stage because they have very low activity in the transesterification reaction [2,4]. The necessity of using two different catalysts in PET production via the DMT process is one of the drawbacks of this process with respect to the TPA process, because in the latter case the prepolymer can be obtained by direct esterification, and only one polycondensation catalyst is necessary.

With the fast growth of the packaging industry, largely using PET to make bottles and other food packagings, great efforts have been made since 1990 to replace the antimony catalysts that have a negative impact on both health and environment [5–8]. Researchers at the Dow Chemical Company have very recently proposed calcined hydrotalcites as safer, efficient catalysts in both stages of PET production [9].

The main aim of this paper is to investigate the use of these basic solids as a catalyst in both DMT transesterification and successive polycondensation. To this end, Al_2O_3, calcined Al–Mg hydrotalcite (CHT1, CHT2, CHT3) with different Al/(Al + Mg) theoretical atomic ratio, and MgO (MgO(I)) were prepared. All the prepared catalysts and a commercial MgO (MgO(II)) were tested in transesterification reactions and characterised. Moreover, a calcined Al–Mg hydrotalcite

* Corresponding author. Tel.: +39-081-674027; fax: +39-081-674026.
E-mail address: santacesaria@chemistry.unina.it (E. Santacesaria).

1381-1169/$ – see front matter © 2003 Elsevier B.V. All rights reserved.
doi:10.1016/j.molcata.2003.10.032

Nomenclature

K_1	kinetic constant of the reaction of a methyl group with a hydroxyl of ethylene glycol (dm^6/(mol min g catalyst))
K_2	kinetic constant of the methyl groups' reaction with a hydroxyl terminating a chain (dm^6/(mol min g catalyst))
K_{e1}	equilibrium constants of the reaction of a methyl group with a hydroxyl of ethylene glycol
K_{e2}	equilibrium constant of the methyl groups' reaction with a hydroxyl terminating a chain
W_{CAT}	catalyst concentration (g/dm^3)

(CHT2) and a commercial MgO (MgO(II)) were also used as single catalysts to produce PET from DMT. The obtained results are reported and discussed in the present work.

2. Experimental

2.1. Materials

Al_2O_3, calcined Al–Mg hydrotalcites with different Al/(Al + Mg) theoretical atomic ratios (CHT1 = 0.33, CHT2 = 0.25), and MgO (MgO(I)) were prepared following the method described by McKenzie and Fishel [10].

The catalysts were prepared mixing two solutions: A, containing $Mg(NO_3)_2$ and $Al(NO_3)_2$ 1.0 M in Al + Mg and different Al/(Al + Mg) atomic ratios; B, prepared dissolving NaOH and Na_2CO_3 (see [10] for details). Solution A was fed at a rate of 1 cm^3/min for 4 h under vigorous stirring, while solution B was fed over time, when it was necessary, to keep the pH 10.

The obtained gels were aged at 338 K for 24 h, and then filtered and washed to pH 7. After drying at 358 K for 14 h, the catalysts were obtained by calcination at 773 K in air for 14 h.

The commercial MgO (MgO(II) was supplied by Merck. All other employed reagents (when not specified) were supplied by Aldrich and used as received without further purification.

2.2. Catalyst characterisations

The elemental compositions of the calcined hydrotalcite catalysts (CHT1, CHT2) were analysed by atomic absorption using a Varian Spectra 220 apparatus. The sulphate content on MgO catalysts was analysed by ionic chromatography using a Metrohm apparatus.

The textural properties of solids were determined using nitrogen adsorption–desorption isotherms at liquid nitrogen temperature by means of a Sorptomatic 1990 instrument. Surface areas were calculated by the BET procedure.

X-ray investigation of the solids was carried out using a Philips 1887 diffractometer. The patterns were run with Cu Kα radiation (λ = 1.5418 Å) at 40 kV and 40 mA; the diffraction angle 2θ was scanned at a rate of 2°/min. The crystallite size was determined by XRD signal width.

Basic properties of the solids were determined by temperature programmed desorption using a TPD/R/O 1100 TermoQuest, with carbon dioxide as the probe molecule [11]. The catalysts were degassed by heating at 773 K under helium and then treated at room temperature with CO_2 stream. Weakly bonded CO_2 was then removed by flushing He. The basic strength distribution were evaluated from the capacity of the material to retain CO_2 during desorption at increasing temperatures (3 K/min).

2.3. Transesterification reaction

Kinetic runs were carried out in a glass reactor fitted with a distillation system able to remove the released methanol. Fifty grams of DMT were put in the reactor and heated at the reaction temperature (180 °C), then an appropriate amount of EG was added to keep the ratio EG/DMT = 2.44. Finally, the catalyst was added. Samples of the reaction mixture were withdrawn at different reaction times and subjected to HPLC analysis.

The HPLC analyses were carried out with a JASCO/PV 980 apparatus and an UV JASCO 975 detector operating at 254 nm, using a Labservice Analytica Spherisorb S5W column (25 cm length, 0.46 cm i.d. silica, 5 μm). The mobile phase fed to the column was a mixture of hexane and dioxane with the composition changing over time according to a scheduled program. More information on the employed analytical method is reported in a previous paper [1].

2.4. Synthesis of PET

The synthesis of PET was carried out in a 30 l jacketed stainless steel reactor. DMT and EG (supplied by Montefibre Co.) were loaded into the reactor. When the reaction mixture reached 180 °C the catalyst was added. Then the temperature was raised to 230 °C and maintained at this value until more than 95% of the theoretical amount of methanol was distilled off.

The pressure was reduced to 0.3 mbar and the temperature was raised to, and maintained at, 290 °C, for 1.5 h. After this the molten PET was extruded by pressurised nitrogen gas and solidified in chilled water.

The intrinsic viscosity of the PET was measured in *o*-chlorophenol at 30 °C using a Ubblohde viscometer. The determination of diethylene glycol content was obtained by PET depolymerisation via methanolysis catalysed by Zn acetate. After the removal of the precipitate, the released diethylene glycol was measured by gas chromatography

(GC–FID) using a 30 m capillary column (0.53 mm i.d.) Supelcowax 20M.

Carboxyl terminal groups were determined by titration using an alcohol solution of KOH and bromophenol-blue as indicator. Samples of PET were dissolved and titrated in orthocresol at 90 °C.

3. Results and discussion

3.1. Catalyst characterisations

Chemical compositions of catalysts, reported in Table 1, are quite close to those of the preparation solutions. The concentrations of sulphates were determined in MgO catalysts by ionic chromatography, since the adsorption properties of MgO can be affected by the presence of this anion [12]. The determined concentrations were negligible for both catalysts ($SO_4^{2-} < 20$ mg/kg).

The X-ray diffraction patterns of the obtained catalysts after calcination at 500 °C are shown in Fig. 1. The Al_2O_3 pattern shows the presence of the γ-alumina phase, while in the MgO(I) pattern the periclase phase is observed [13]. In the case of Mg/Al systems (CHT1, CHT2), only the presence of an MgO-like phase is observed [13]. From the data in Table 1, we can see that higher surface areas and smaller crystallites are favoured by Al contents in CHT samples with respect to MgO(I), in agreement with data reported by Di Cosimo et al. [11].

CO_2-TPD profiles for all the catalysts are shown in Fig. 2. The complex desorption profiles are due to the presence of basic sites of different strengths. In particular, all solids have a desorption peak at temperatures around 100 °C, which can be attributed to the interaction with sites having weak basic strengths [11,13]. A second desorption peak attributed to medium basic sites can be seen clearly for $T \approx 200$–250 °C in the case of CHT2 and MgO(I). Observing the CO_2 desorption profile of CHT1 at the same temperatures a variation in the curve gradient can be seen. This behaviour can be due to the presence, on this catalyst also, of basic sites of medium strength at a lower concentration, in agreement with lower Mg content. The two magnesium oxides show another low desorption peak at $T \approx 450$ °C which can be attributed to the stronger basic sites on the surface. The intrinsic basicity measured by CO_2-TPD also varied with samples.

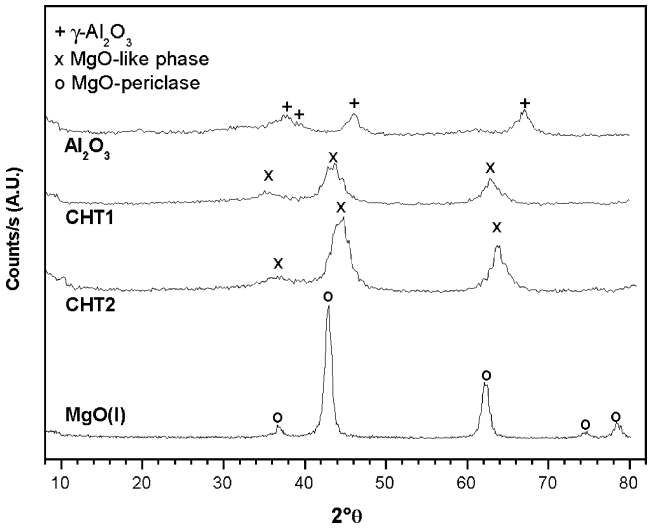

Fig. 1. X-ray diffraction patterns of catalysts.

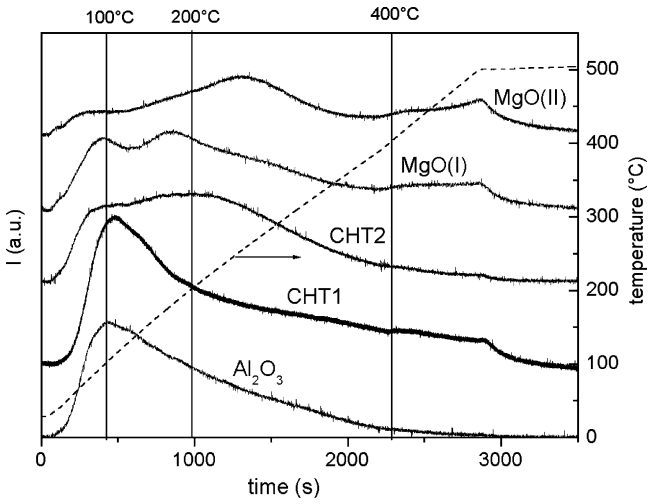

Fig. 2. CO_2-TPD profiles of catalysts.

The lowest intrinsic basicity was found on Al_2O_3, while, the CHT and MgO(I) samples have very similar values. It is interesting to observe that in MgO(II) sample, intrinsic basicity strongly increase with respect to MgO(I) despite the decrease of surface are. This means that surface density of basic sites can strongly be affected by the preparation

Table 1
Characterisation of CHT and MgO for chemical composition, BET surface area, pore volume, crystallite size, overall CO_2 adsorbed

Catalyst	Al/(Al + Mg)		Surface (m^2/g)	Pore volume (cm^3/g)	Crystallite size (Å)	Specific basicity (μmol/g)	Intrinsic basicity (μmol/$m^)$
	Theoretical	Experimental					
Al_2O_3	1	–	358	0.48	20	322	0.9
CHT1	0.33	0.40	182	1.08	32	473	2.6
CHT2	0.25	0.22	138	0.94	29	373	2.7
MgO(I)	0	–	134	0.44	77	348	2.6
MgO(II)	0	–	36	0.15	115	266	7.4

Table 2
Operative conditions of transesterification runs and the corresponding kinetic parameters obtained by mathematical regression analysis

Run	Catalyst	Temperature (°C)	EG/DMT (mol/mol)	Catalyst/DMT (g/g, 10^4)	K_1 (dm^6/(mol min g catalyst))	K_2 (dm^6/(mol min g catalyst))	S_1
A1	Al_2O_3	180	2.44	4.0	–	–	–
A2	CHT1	180	2.44	4.0	0.0100 ± 0.0001	0.0026 ± 0.0001	0.79
A3	CHT2	180	2.44	4.0	0.0173 ± 0.0002	0.0051 ± 0.0002	0.77
A5	MgO(I)	180	2.44	2.3	0.0445 ± 0.0006	0.0105 ± 0.0004	0.81
A6	MgO(II)	180	2.44	2.2	0.0829 ± 0.0021	0.0236 ± 0.0016	0.78

method. The observed increase of specific basicity with the decrease of surface area for MgO is in agreement with data reported by other authors [10,14].

3.2. Transesterification reaction

The list of transesterification runs with the corresponding operative conditions is reported in Table 2. In Figs. 3 and 4, the results of the HPLC analysis for runs A3 and A5 of Table 2 are shown as examples.

The transesterification of DMT with EG occurs with the formation of many oligomers characterised by the different terminal groups of the chains, which can be hydroxyl–hydroxyl, methyl–hydroxyl or methyl–methyl such as in the following reactions [1,2,15]:

$$X_n = H_3C–[OOC–\phi–COOC_2H_4]_i–OOC–\phi–COOCH_3 \quad (i = 0, n) \tag{1}$$

$$Y_n = HOC_2H_4–[OOC–\phi–COOC_2H_4]_i–OH \quad (i = 0, n) \tag{2}$$

$$Z_n = HOC_2H_4–[OOC–\phi–COOC_2H_4]_i–OOC–\phi–COOCH_3 \quad (i = 0, n) \tag{3}$$

where X_0 corresponds to DMT; Y_0 to EG; Z_1 to methyl hydroxyethyl terephthalate (MHET); Y_1 to bis(2-hydroxyethyl) terephthalate, which is the main product, etc.

These products originate from the possibility of many simultaneous and consecutive reactions, as shown in Fig. 5, where, for simplicity, only three stages of reactions have been considered and the formation of methanol is not reported.

Kinetic runs of transesterification reactions have been interpreted with a mathematical model based on the classical definition of the complex reaction scheme that was developed in previous papers [1,2]. A four-stage model was employed involving 24 different oligomers and 58 reactions. All the reactions considered and the related kinetic laws are reported in Table 3. Despite the large number of oligomers and of the occurring reactions, only two kinetic constants and two equilibrium constants are necessary to describe the system. The first set of kinetic (K_1) and equilibrium (K_{e1}) constants is related to the reaction of a methyl group with a hydroxyl of ethylene glycol, while the second corresponds

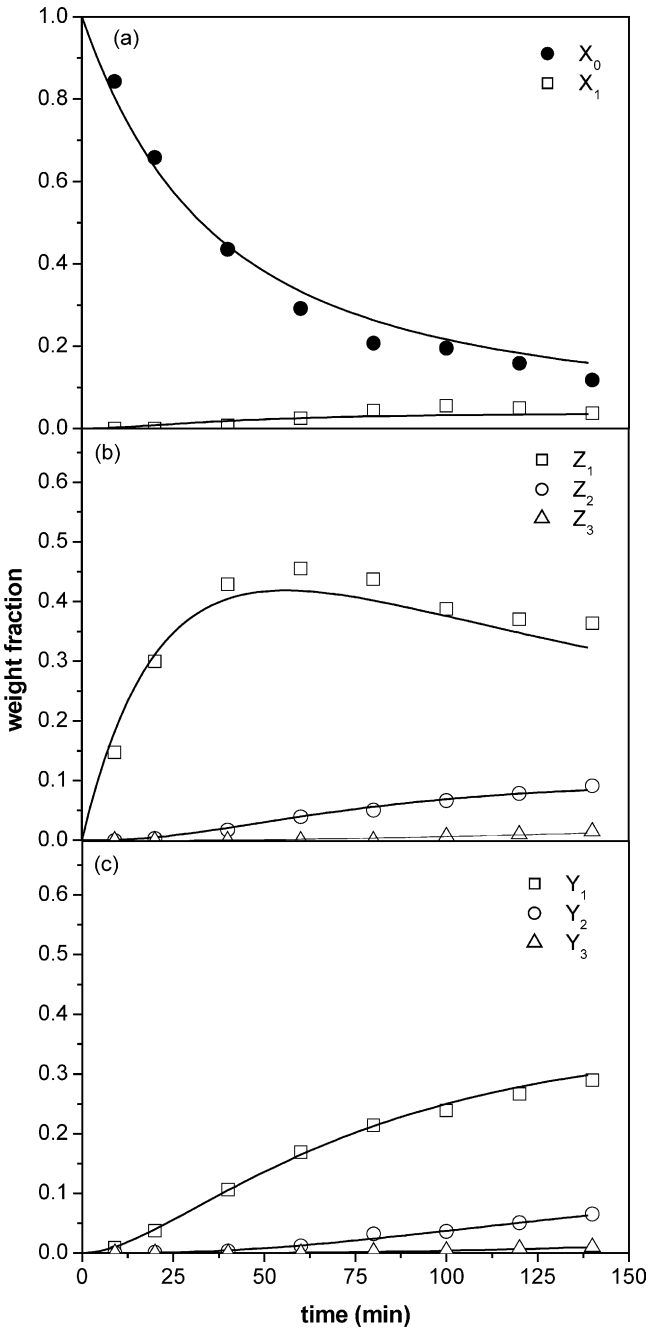

Fig. 3. Example of the agreement obtained between experimental and calculated oligomers distribution of type X (a), Y (b) and Z (c), respectively, for the kinetic run A3 of Table 2. Lines are calculated data, and symbols the experimental data.

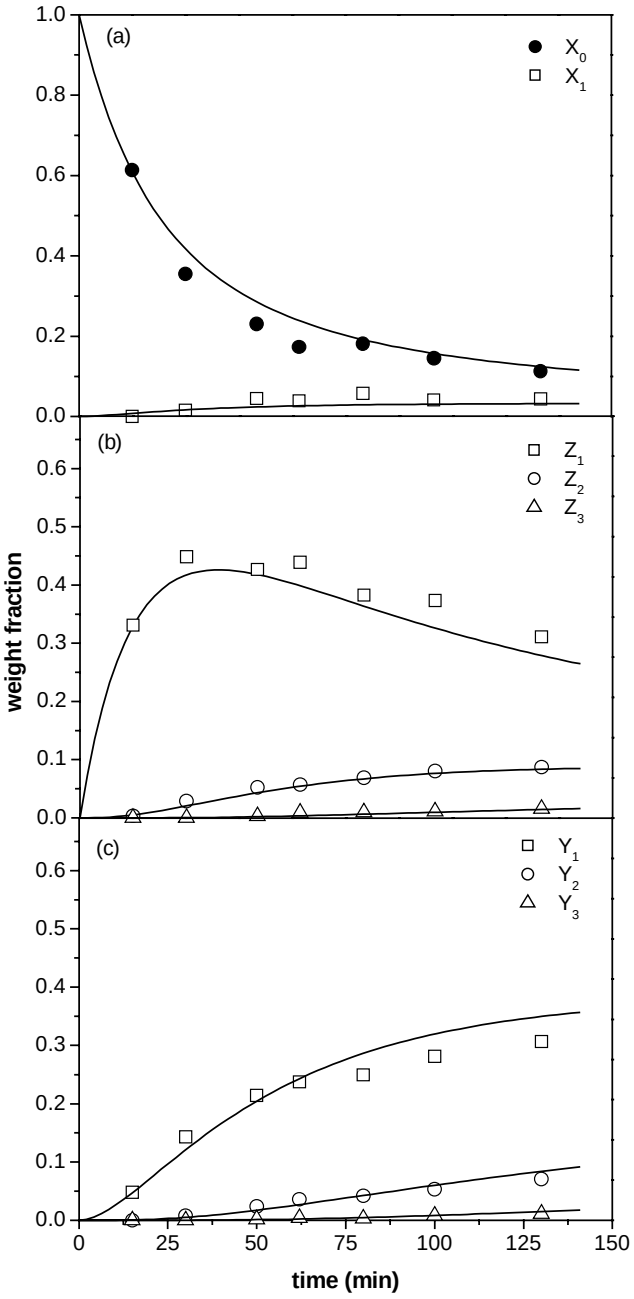

Fig. 4. Example of the agreement obtained between experimental and calculated oligomers distribution of type X (a), Y (b) and Z (c), respectively, for the kinetic run A5 of Table 2. Lines are calculated data, and symbols the experimental data.

to the kinetic (K_2) and equilibrium (K_{e2}) constants of the methyl groups' reaction with a hydroxyl terminating a chain. The related selectivity of these two reactions can be simply expressed as: $S_1 = K_1/(K_1 + K_2)$. It was shown that a high S_1 selectivity gives a high concentration of Y-type oligomers which are the most reactive in the polymerisation reaction with a classical polycondensation catalyst [2]. More details on the kinetic and mathematical model can be found in the mentioned papers [1,2].

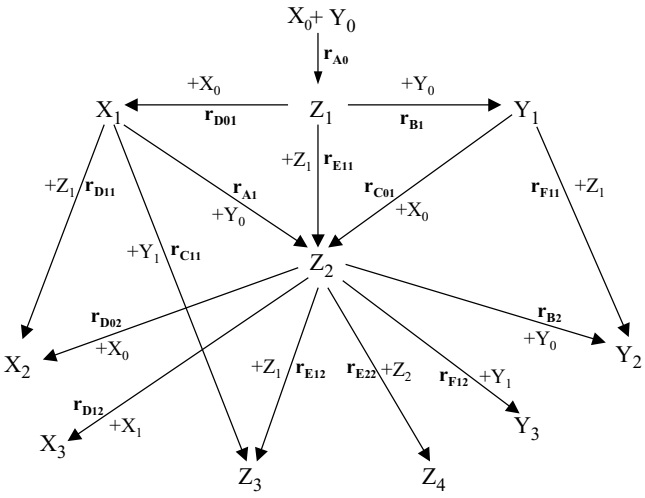

Fig. 5. Reaction scheme truncated at the third stage.

The values of K_1 and K_2 were obtained submitting the experimental data related to the runs of Table 2 to mathematical regression analysis [16], applying the cited kinetic model. In the simulations, the values of the corresponding equilibrium constants were set equal to those obtained in a previous paper for the same temperature reaction ($K_{e1} = 0.28$; $K_{e2} = 0.21$) [2].

The values of constants K_1 and K_2 obtained by regression analysis are also reported in Table 2, while two examples of the agreement obtained can be evaluated in Figs. 3 and 4.

The first observation is that the specific activities of catalysts, which are related to the transesterification kinetic constants of Table 2, increase along with Al/(Al + Mg) ratios (runs A1–A4). In fact, Al_2O_3 is inactive in the reaction, while the transesterification specific activity is in the order

Table 3
kinetic equations applied to the model

Types of reactions

(Ai) $X_i + Y_0 \Leftrightarrow Z_{i+1} + CH_3OH \quad (i = 0, 3)$

(Bi) $Z_i + Y_0 \Leftrightarrow Y_i + CH_3OH \quad (i = 0, 4)$

(Cij) $X_i + Y_j \Leftrightarrow Z_{i+j+1} + CH_3OH \quad (i = 1, 3;\ j = 1, 3)$

(Dij) $X_i + Z_j \Leftrightarrow X_{i+j} + CH_3OH \quad (i = 1, 3;\ j = 1, 4)$

(Eij) $Z_i + Z_j \Leftrightarrow Z_{i+j} + CH_3OH \quad (i = 1, 4;\ j = 1, 4;\ ij \neq 12, 13, 14, 23, 24, 34)$

(Fij) $Z_i + Y_j \Leftrightarrow Y_{i+j} + CH_3OH \quad (i = 1, 4;\ j = 1, 3)$

Corresponding kinetic equations

$$r_{Ai} = K_1 W_{CAT}[X_i][Y_0] - \frac{K_1}{K_{e1}} W_{CAT}[Z_{i+1}][CH_3OH]$$

$$r_{Bi} = \frac{K_1}{2} W_{CAT}[Z_i][Y_0] - \frac{K_1}{2K_{e1}} W_{CAT}[Y_i][CH_3OH]$$

$$r_{Cij} = K_2 W_{CAT}[X_i][Y_j] - \frac{K_2}{K_{e2}} W_{CAT}[Z_{i+j+1}][CH_3OH]$$

$$r_{Dij} = \frac{K_2}{2} W_{CAT}[X_i][Z_j] - \frac{K_2}{2K_{e2}} W_{CAT}[X_{i+j}][CH_3OH]$$

$$r_{Eij} = \frac{K_2}{2} W_{CAT}[Z_i][Z_j] - \frac{K_2}{2K_{e2}} W_{CAT}[Z_{i+j}][CH_3OH]$$

$$r_{Fij} = \frac{K_2}{2} W_{CAT}[Z_i][Y_j] - \frac{K_2}{2K_{e2}} W_{CAT}[Y_{i+j}][CH_3OH]$$

Table 4
Operative conditions of the polycondensation runs and the intrinsic viscosity, diethylene glycol content, and carboxyl terminal groups of the obtained polymers

Run	Catalyst	EG/DMT (mol/mol)	Catalyst/DMT (g/g, 10^4)	Intrinsic viscosity (dl/g)	DEG (wt.%)	[COOH] (meq./kg)
B1	CHT2	2.0	1.2	0.56	0.96	0.47
B2	MgO(II)	2.0	0.6	0.57	1.08	0.44
	Classical catalytic system [17]	–	–	>0.60	0.7–0.80	0.40–0.60

CHT1 < CHT2 < MgO(I). This is in agreement with data reported by Corma et al. for the glycerolysis of fats [17]. This behaviour does not follows the values of the specific basicity of the solids. In fact, these have an inverse trend, lowering in the order CHT1 > CHT2 > MgO. Therefore, the specific activity can be related to the presence of medium and strong basic sites on the catalysts surface. In fact, these sites are absent on Al_2O_3 that not show any activity, while, their concentrations increase along with the decrease of the Al/(Al + Mg) ratio, and consequently activities increase, too. Moreover, for the same reason the specific activity of MgO(I) is greater than the activity of MgO(II).

However, it is interesting to observe that despite the fact that MgO(I) and MgO(II) have the same chemical composition, and crystalline structure, these two catalysts have different intrinsic activities, reflecting the different intrinsic basicity reported in Table 1. In fact, for MgO(I) we can calculate for DMT transesterification an intrinsic constant $K_1' = 0.62 \times 10^{-3}\,dm^6/(mol\,m^2)$, while in the case of MgO(II) we have an higher value of $K_1' = 1.24 \times 10^{-3}\,dm^6/(mol\,m^2)$. The higher intrinsic activity of MgO(II) is clearly related to the higher intrinsic basicity, as mentioned before. The observation that MgO catalyst with lower surface area have higher intrinsic activity and intrinsic basicity is in agreement with the observation of Bancquart et al. [14], and can also be derived from the work of Coluccia and co-workers [18]. Coluccia and co-workers [18] have pointed out that the properties of MgO strongly depend on the preparation method, this by using high-resolution transmission electron microscopy and FTIR spectroscopy. Studying two different MgO catalysts, that is, a MgO-h (surface area = $200\,m^2/g$) obtained by thermal decomposition of parental hydroxide and a MgO-sa (surface area = $95\,m^2/g$), a commercial smoke powder, obtained by burning magnesium in air, they found that the solid with the higher surface area has the higher concentration per gram of catalysts of the $(Mg^{2+})_{LC}(O^{2+})_{LC}$ pairs in lowest co-ordination, that are the most basic sites. From the same work, it is also possible to derive an increase in the intrinsic basicity with the lowering of MgO surface area. This observation can be derived from Fig. 6 of the cited paper [18]. In this figure, the IR spectra of D_2 adsorbed at room temperature on, respectively, MgO-h and MgO-sa in the presence of 0.26 bar D_2, are reported. The detected signals are related to the presence of $(Mg^{2+})_{LC}(O^{2+})_{LC}$. From this figure, we have calculated the ratio between the IR signal integrations I_1(MgO-h)/I_2(MgO-sa), corresponding to the ratio of $(Mg^{2+})_{LC}(O^{2+})_{LC}$ concentrations on the two different MgO. The obtained experimental value of the I_1(MgO-h)/I_2(MgO-sa) ratio is 1.7. If the intrinsic concentration of strong basic sites does not depend on surface area, the I_1(MgO-h)/I_2(MgO-sa) ratio should be equal to the ratio of surface area S_1(MgO-h)/S_2(MgO-sa), which is 2.1 instead of 1.7. Hence, the intrinsic concentration of strong basic sites on MgO-sa is higher than the one on MgO-h. This result agrees with our observation that both intrinsic basicity and intrinsic activity increase by decreasing MgO surface area.

3.3. Synthesis of PET

The list of the polycondensation runs performed with the corresponding operative conditions and measured values of intrinsic viscosity, diethylene glycol content, and carboxyl terminal groups of obtained polymers are reported in Table 4. Moreover, in Table 4, the values of chemical characterisations of typical polymers obtained by classical catalysts are reported too [19]. As can be seen, the results for both catalysts are very promising. In fact, the obtained polymers have characteristics very similar to the commercial polymers, despite the fact that their synthesis was not optimised concerning the choice of operative conditions and additive use.

4. Conclusion

The CHT and MgO catalysts are active in the transesterification reaction of DMT with EG. It is noteworthy that in all cases the prepared active catalysts have about the same activities than those of classical catalysts (K_1 = 0.02–0.08 $dm^6/(mol\,g\ catalyst)$; and selectivities are comparable to those of the best classical catalysts (S_1 = 0.7–0.8) [2].

The activity of transesterification reactions is related to the concentration of medium and strong basic sites, which increase along with the decrease of the Al/(Al + Mg) ratio. The intrinsic activity of MgO is not constant and increases along with the decrease in the specific surface areas because the increase of intrinsic basicity. Since the obtained specific and intrinsic basicity is strictly related to the MgO preparation method [10,14,18,20], improvement in the performance of MgO based catalysts could be achieved by improving theses methods. These aspects will be studied in the near future.

It was confirmed, moreover, that the calcined Al–Mg hydrotalcite can be used as a single catalyst in PET production from DMT and it was shown that MgO also is a useful catalyst for this purpose.

Since MgO has higher activities in both transesterification and polycondensation reactions and is much more simple to prepare compared to calcined hydrotalcite, it seems to be the best single catalyst in PET production.

Acknowledgements

The authors wish to thank S. Contessa (Montefibre SpA) for the polymerisation tests and characterisation of polymers and Dr. M. Trifuoggi for some analytical determinations.

References

[1] E. Santacesaria, F. Trulli, L. Minervini, M. Di Serio, R. Tesser, S. Contessa, J. Appl. Polym. Sci. 54 (1994) 1371.
[2] M. Di Serio, R. Tesser, F. Trulli, E. Santacesaria, J. Appl. Polym. Sci. 62 (1996) 409.
[3] R. Lasarova, K. Dimov, Angew. Makromol. Chem. 55 (1976) 1.
[4] H. Köpnick, M. Schmidt, W. Brügging, J. Rüter, W. Kaminsky, in: W. Gerhartz, et al. (Eds.), Ullmann's Encyclopedia of Industrial Chemistry, vol. A21, 5h ed., VCH, Weinheim, 1992, p. 227.
[5] U.K. Thiele, Int. J. Polym. Mater. 50 (2001) 387.
[6] U. Meyer, W.F. Hoelderich, Appl. Catal. A: Gen. 178 (1999) 159.
[7] H. Gorzawski, W.F. Hoelderich, Appl. Catal. A: Gen. 179 (1999) 131.
[8] J.P. Wingner, V. Voerckel, S. Munjal, R. Eckert, G. Feix, M. Sela, WO 01/42335 A1 (2001).
[9] H. Staeuber, V. Voerckel, J. Wiegner, WO 03/004547 (2003).
[10] A.L. McKenzie, C.T. Fishel, R.J. Davis, J. Catal. 138 (1992) 547.
[11] J.I. Di Cosimo, V.K. Díez, M. Xu, E. Iglesia, C.R. Apesteguía, J. Catal. 178 (1998) 499.
[12] J. Wang, J.A. Lercher, G.L. Haller, J. Catal. 88 (1984) 18.
[13] M. Bolognini, F. Cavani, D. Scagliarini, C. Flego, C. Perego, M. Saba, Catal. Today 75 (2002) 103.
[14] S. Bancquart, C. Vanhove, Y. Pouilloux, J. Barrault, Appl. Catal. A: Gen. 218 (2001) 1.
[15] J.M. Besnoin, G.D. Lei, K.Y. Choi, AIChE J. 35 (1989) 1445.
[16] G. Buzzi-Ferraris, Analisi ed Identificazione dei Modelli, CLUP, Milano, 1975.
[17] A. Corma, S. Iborra, S. Miquel, J. Primo, J. Catal. 173 (1998) 315.
[18] G. Martra, T. Cacciatori, L. Marchese, J.S.L. Hargreaves, I.M. Mellor, R.W. Joyner, S. Coluccia, Catal. Today 70 (2001) 121.
[19] S. Contessa, private communication.
[20] V.R. Choudary, M.Y. Pandit, Appl. Catal. 71 (1991) 265.